Engineered Human Skin Substitutes Undergo Large-Scale Genomic Reprogramming and Normal Skin-Like Maturation after Transplantation to Athymic Mice

Jennifer M. Klingenberg[1], Kevin L. McFarland[1], Aaron J. Friedman[2], Steven T. Boyce[1,3], Bruce J. Aronow[2] and Dorothy M. Supp[1,3]

Bioengineered skin substitutes can facilitate wound closure in severely burned patients, but deficiencies limit their outcomes compared with native skin autografts. To identify gene programs associated with their *in vivo* capabilities and limitations, we extended previous gene expression profile analyses to now compare engineered skin after *in vivo* grafting with both *in vitro* maturation and normal human skin. Cultured skin substitutes were grafted on full-thickness wounds in athymic mice, and biopsy samples for microarray analyses were collected at multiple *in vitro* and *in vivo* time points. Over 10,000 transcripts exhibited large-scale expression pattern differences during *in vitro* and *in vivo* maturation. Using hierarchical clustering, 11 different expression profile clusters were partitioned on the basis of differential sample type and temporal stage-specific activation or repression. Analyses show that the wound environment exerts a massive influence on gene expression in skin substitutes. For example, *in vivo*–healed skin substitutes gained the expression of many native skin-expressed genes, including those associated with epidermal barrier and multiple categories of cell–cell and cell–basement membrane adhesion. In contrast, immunological, trichogenic, and endothelial gene programs were largely lacking. These analyses suggest important areas for guiding further improvement of engineered skin for both increased homology with native skin and enhanced wound healing.

Journal of Investigative Dermatology (2010) **130,** 587–601; doi:10.1038/jid.2009.295; published online 1 October 2009

INTRODUCTION

The gold standard for closure of excised full-thickness burns is autografting with full-thickness or split-thickness skin grafts. Autografts are harvested from uninjured areas of the patient's skin, and split-thickness autografts may be reharvested after healing to provide sufficient grafts to complete wound closure. In patients with very large total body surface area wounds, insufficient donor sites for autografting complicate wound closure, which can compromise recovery, increase the risk of invasive wound infection and mortality (Wolf *et al.*, 1997; Xiao-Wu *et al.*, 2002), and contribute to excessive scarring (Garner, 1998). The need for permanent wound closure in burn patients has driven the development of autologous engineered skin replacements. The most important function of a skin substitute is the restoration of barrier function, but skin substitutes should also replace both dermis and epidermis, achieve functional and cosmetic results similar to autograft and native human skin (NHS), and reduce the requirements for surgical procedures. No skin substitutes are currently available that meet all of these requirements; however, cultured skin substitutes (CSS) comprised of cultured autologous keratinocytes, fibroblasts, and biopolymers meet some of these goals (Boyce *et al.*, 2006). For example, although the epidermal barrier of CSS *in vitro* is deficient compared with that of NHS, CSS approximate the barrier properties of NHS by 6 weeks after grafting (Barai *et al.*, 2007). Further, CSS were shown to significantly reduce the amount of autograft harvesting required for wound closure in patients with >50% total body surface area burns, thereby reducing the number of surgical procedures required (Boyce *et al.*, 2006). However, despite encouraging clinical results, limitations in anatomy and physiology of CSS remain, including lack of a vascular

[1]*Research Department, Shriners Hospitals for Children—Cincinnati, Cincinnati, Ohio, USA;* [2]*Computational Medicine Center and Division of Biomedical Informatics, Cincinnati Children's Hospital Medical Center, Cincinnati, Ohio, USA and* [3]*Department of Surgery, University of Cincinnati College of Medicine, Cincinnati, Ohio, USA*

Correspondence: Dr Dorothy M. Supp, Research Department, Shriners Hospitals for Children—Cincinnati, 3229 Burnet Avenue, Cincinnati, Ohio 45229, USA. E-mail: dsupp@shrinenet.org

Abbreviations: Ab, antibody; CSS, cultured skin substitute; ER, endoplasmic reticulum; KRT15, keratin 15; KRT2, keratin 2; LOR, loricrin; NHS, native human skin

Received 27 February 2009; revised 1 July 2009; accepted 24 July 2009; published online 1 October 2009

plexus (Boyce *et al.*, 1995), which has been demonstrated in other preclinical models (Tremblay *et al.*, 2005) but not in engineered skin transplanted to humans.

Comparisons of global gene expression profiles of engineered tissues and native tissues can provide measures of homology and can also be used to identify deficiencies. Previous studies analyzed gene expression in CSS, in constituent cell populations (primary human fibroblasts and keratinocytes), and in NHS, using complementary DNA microarrays. Those studies demonstrated that CSS *in vitro,* at the time of transplantation, exhibit a hyperproliferative phenotype consistent with healing human skin (Smiley *et al.*, 2005a). This study increases our understanding of gene expression patterns that guide the development of CSS *in vitro* and characterizes the expression changes that occur after grafting. A comprehensive analysis of gene expression profiles of CSS at multiple time points reveals the dynamic interactions between fibroblasts and keratinocytes during *in vitro* maturation, as well as the marked changes that occur after transplantation *in vivo*. A comparison with the gene expression profile of NHS highlights the pathways that are deficient in healed CSS, which can guide further engineering of CSS for greater homology with normal skin.

RESULTS

Preparation of engineered skin grafts and transplantation to athymic mice

Primary human keratinocytes and fibroblasts isolated from two distinct adult skin donors were used separately to prepare CSS for grafting to mice. Biopsy samples of CSS were collected at days 3, 7, and 14 of *in vitro* incubation for RNA isolation and histological examination (Figure 1a–c), and at day 14, CSS were transplanted to full-thickness wounds in athymic mice. Mice were killed and biopsy samples were collected for analysis at 3, 7, 14, 28, 42, and 56 days after grafting (Figure 1d–i). For each time point analyzed, both original skin donors were represented.

At 3 days after transplantation, grafts were loosely adhered to the wound bed but not to wound margins (data not shown). Histological sections revealed a very thin epidermal layer with accumulation of cornified material (Figure 1d), possibly because of occlusion by wound dressings. Within 1 week, grafts were found to be well adhered to the wound bed and wound margins had partially healed (Figure 2a). At this stage, a thin epidermis was apparent (Figure 1e), and graft surfaces appeared wet, indicating an incomplete barrier function. Within 2 weeks of grafting, CSS were found to be well adhered to wound beds and wound margins (Figure 2b). Hyperkeratotic plaques were present at graft surfaces because of the accumulation of stratum corneum beneath the dressing material; these plaques were easily peeled off the grafts at day 14, revealing a uniformly dry epithelial surface. Between weeks 2 and 6, grafted areas tended to contract slightly and then stabilized between weeks 6 and 8 after grafting. Spots of pigment, resulting from randomly localized passenger melanocytes present nonspecifically in epidermal cell cultures, were observed at 4 weeks after grafting of CSS, and the sizes of pigmented regions expanded through 8 weeks after grafting (Figure 2c–f). The number of foci per graft and the level of pigment varied according to the original skin donor (Figure 2d and e).

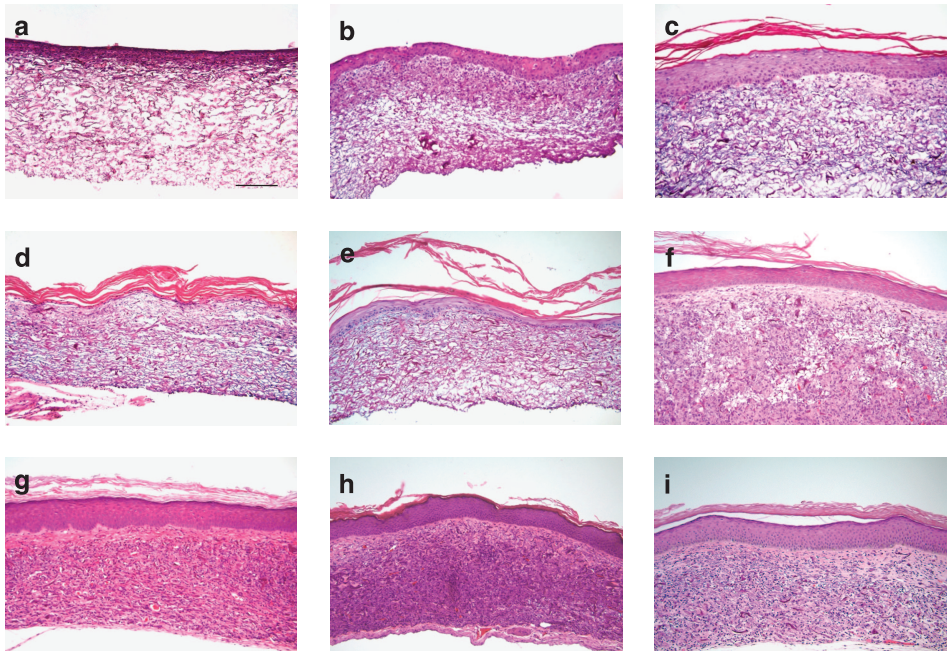

Figure 1. Histological sections of engineered skin *in vitro* and *in vivo*. Representative formalin-fixed, paraffin-embedded, hematoxylin and eosin–stained sections from the time points studied by microarray analysis are shown. (**a**) *In vitro* incubation day 3. (**b**) *In vitro* incubation day 7. (**c**) *In vitro* incubation day 14. (**d**) 3 Days after grafting to mice *in vivo*. (**e**) 7 Days after grafting. (**f**) 14 Days after grafting. (**g**) 28 Days after grafting. (**h**) 42 Days after grafting. (**i**) 56 Days after grafting. Scale bar shown in panel (**a**) is for all panels (0.2 mm).

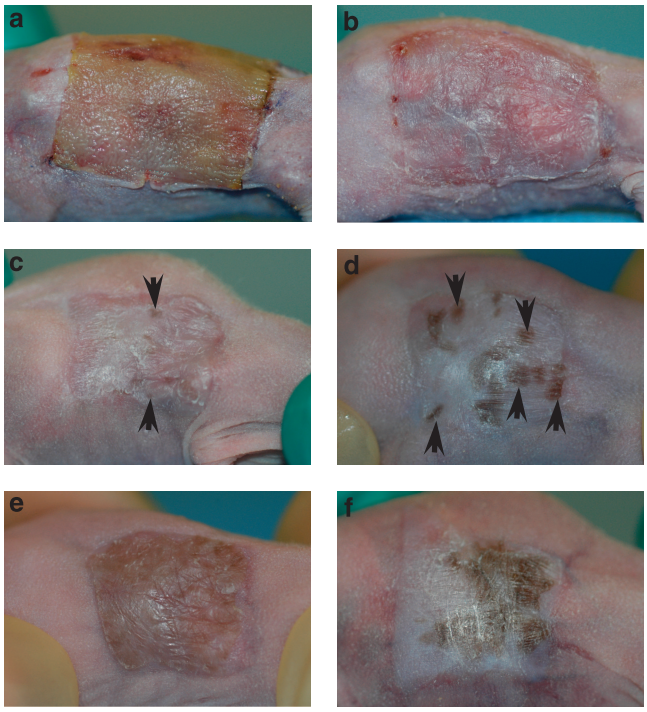

Figure 2. Healing of CSS grafted to athymic mice. Photographs were taken at 7 (**a**), 14 (**b**), 28 (**c**), 42 (**d**, **e**), and 56 days (**f**) after grafting. Different animals are shown in each panel. Note pigmented areas (arrows in **c**, **d**) resulting from passenger melanocytes that are first noticeable within 28 days of grafting. Both the density of passenger melanocytes and intensity of pigmentation are donor specific. For example, note the darkly pigmented but well-separated spots in the graft shown in (**d**), compared with the nearly uniform but more lightly pigmented graft in panel (**e**); these grafts were prepared with cells from different skin donors.

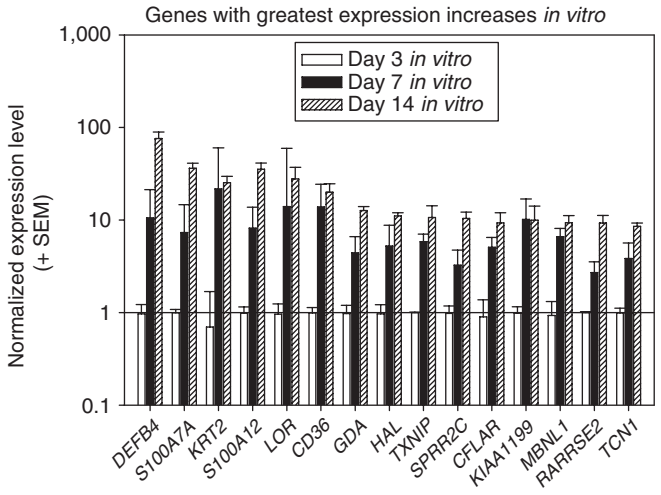

Figure 3. Top 15 upregulated genes in CSS *in vitro*. Genes normally expressed in activated keratinocytes or associated with epidermal differentiation were among the most highly upregulated during *in vitro* morphogenesis of engineered skin. Shown are the mean normalized expression levels for 15 genes with the greatest relative increases from day 3 to day 14 of *in vitro* incubation. Error bars represent standard error of the mean (SEM).

RNA samples isolated from NHS and CSS from multiple stages after *in vitro* and *in vivo* maturation were used for microarray analysis. For analysis of data, we focused on a pool of genes significantly expressed in any of the NHS, CSS *in vitro,* or CSS *in vivo* samples. This initial filtering approach generated a list of 10,359 probe sets that mapped to 6,688 nonredundant genes that were expressed consistently across all samples of at least one group or time point.

Gene expression changes during *in vitro* incubation

Striking changes in gene expression were observed from day 3 through to day 14 of *in vitro* incubation. Many of the genes that were upregulated during *in vitro* morphogenesis of CSS were involved in epidermal differentiation (Figure 3). The largest increase, representing a 78-fold change from day 3 to day 14, was observed for the expression of antimicrobial peptide β-*defensin 2* (*DEFB4* gene). In addition, the differentiation-specific keratin 2 gene (*KRT2*), expressed in the suprabasal layers of normal skin, increased 36-fold in CSS *in vitro*. *CD36*, which is involved in fatty acid transport and is upregulated in keratinocytes after wounding (Simon Jr *et al.*, 1996), was increased 20-fold *in vitro*. Further, four of the top 15 induced genes *in vitro*—*S100 calcium-binding protein A7A* (*S100A7A*), *S100 calcium-binding protein A12* (*S100A12*), *loricrin* (*LOR*), and *small proline-rich protein 2C* (*SPRR2C*)—map to human chromosome 1q21, a region known as the epidermal differentiation complex, which contains a large number of genes with critical roles in epidermal maturation (Mischke *et al.*, 1996).

Gene expression changes after grafting to athymic mice

The transplantation of CSS resulted in massive changes in gene expression. Many of the genes that were most highly upregulated during *in vitro* morphogenesis of CSS were downregulated within 3 days of grafting, including *KRT2, LOR, CD36, DEFB4, transcobalamin I* (*TCN1*), and *guanine deaminase* (*GDA*) (Figure 4a). The expression of most of these genes remains low after grafting, approaching relatively low levels similar to native human skin. However, expression levels of *KRT2*, *LOR*, and *CD36* increase within 1 week of grafting and approach levels similar to native skin between 2 and 4 weeks after grafting (Figure 4a).

Other genes were significantly increased immediately after grafting to mice. The greatest fold increase was found for the *SERPINB6* gene, which encodes a serine proteinase inhibitor that is increased in keratinocytes on differentiation (Scott *et al.*, 1998). Furthermore, expression is highly increased for the *LGALS1* gene, which encodes the β-galactoside-binding lectin, galectin-1. *Sterol carrier protein-2* (*SCP2*), which is involved in phosphatidylinositol signaling (Schroeder *et al.*, 2003), was increased after grafting and remained high compared with NHS; this gene has not been previously described in skin. *Four-and-a-half lim domains 1* (*FHL1*), a putative stem cell marker protein, was induced in CSS on grafting, as was the *inhibitor of DNA binding 2* (*ID2*), a helix-loop-helix protein that negatively regulates cell differentiation and was reported to be expressed in basal keratinocytes (Hammond and Jahoda, 2008).

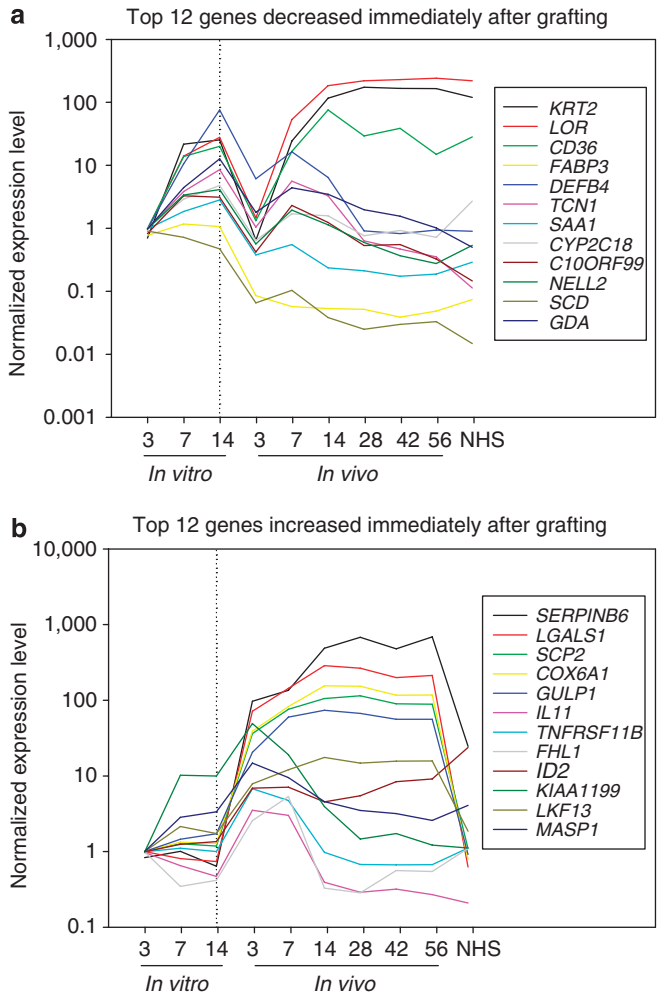

Figure 4. Expression of genes highly downregulated or upregulated immediately after grafting to mice. The ratio of normalized expression at day 14 *in vitro* to day 3 *in vivo* was calculated for each gene, and the genes that showed the greatest decreases (**a**) or increases (**b**) in expression were determined. Mean normalized expression levels (vertical axes) are plotted *versus* sample type (CSS *in vitro*, *in vivo*, or NHS; horizontal axes).

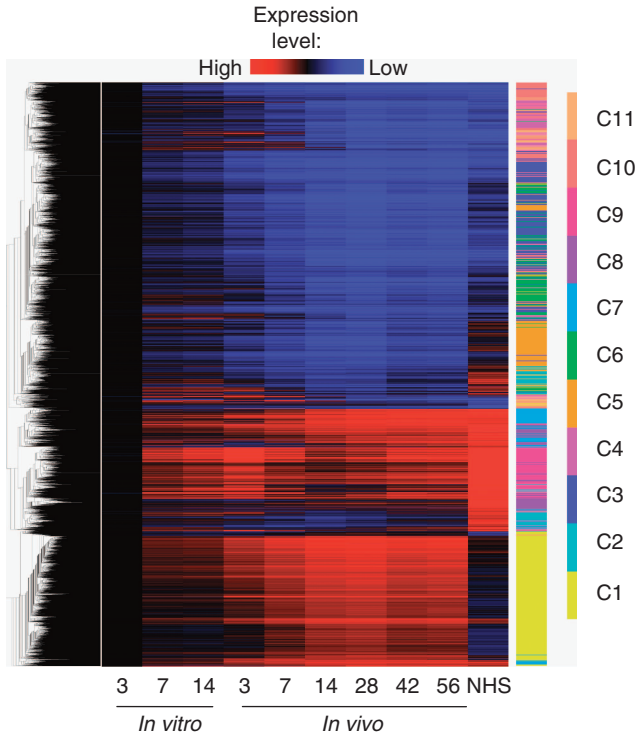

Figure 5. Relative expression of 10,359 probe sets that were differentially regulated in CSS *in vitro* and after grafting. Hierarchical clustering identified 11 different expression profiles that varied by sample type and time. Relative gene expression levels, which were normalized to mean expression at day 3 *in vitro*, are shown. Red represents high expression and blue represents low expression. Transcripts are arrayed vertically, with the hierarchical tree on the left, and the different sample groups are represented on the horizontal axis. Each column represents the mean expression for that sample group. The 11 clusters (C1–C11) are indicated by color coding on the right side of the figure.

Clustering and pathway analysis

To visualize expression patterns, a heat map of the 10,359 probe sets was constructed by referencing each probe set's relative expression during maturation *in vitro* or *in vivo* after grafting to that of the first *in vitro* sample, day 3 of *in vitro* incubation. To gain an overall appreciation of the biological activities engendered by the different coordinately regulated sets of genes, expression patterns were divided into 11 clusters of transcripts using K-means clustering. Each cluster represents an expression behavior that varied by sample type and time (Figure 5). Normalized gene expression levels for the top 100 probe sets in each cluster are presented in Supplementary Table S1. The expression of the top 10 known genes in each cluster, which were ranked on the basis of characteristic expression behaviors, is shown in Figure 6; these plots, which graphically depict expression levels for each time point (CSS *in vitro* and *in vivo*) or sample type (CSS or NHS), provide a general view of the behavior of genes in a given cluster. Each cluster was then subjected to gene set enrichment analysis (Subramanian *et al.*, 2005), as implemented in ToppGene (Chen *et al.*, 2009), to identify biological processes, molecular functions, and cellular components that were significantly associated with each cluster (Supplementary Table S2).

Cluster 1 contains 2,335 probe sets that were expressed at low levels in CSS *in vitro,* increased in CSS at day 7 after grafting, and peaked around the middle of the *in vivo* time course at day 28 after grafting. These genes were all expressed at higher levels in CSS compared with NHS. The genes in this cluster are involved in a variety of functions, including ion transport, channel activity, and developmental processes (Supplementary Table S2). Pathway analysis revealed multiple functional categories involving development, which were significantly associated with the cluster 1 expression pattern. For example, of the 1,751 nonredundant genes in cluster 1, there are 270 genes involved in Multicellular Organismal Development (Biological Process GO:0007275; Supplementary Table S2). These include 15 different genes of the homeobox (HOX) transcription factor family, which are considered master regulators of embryonic

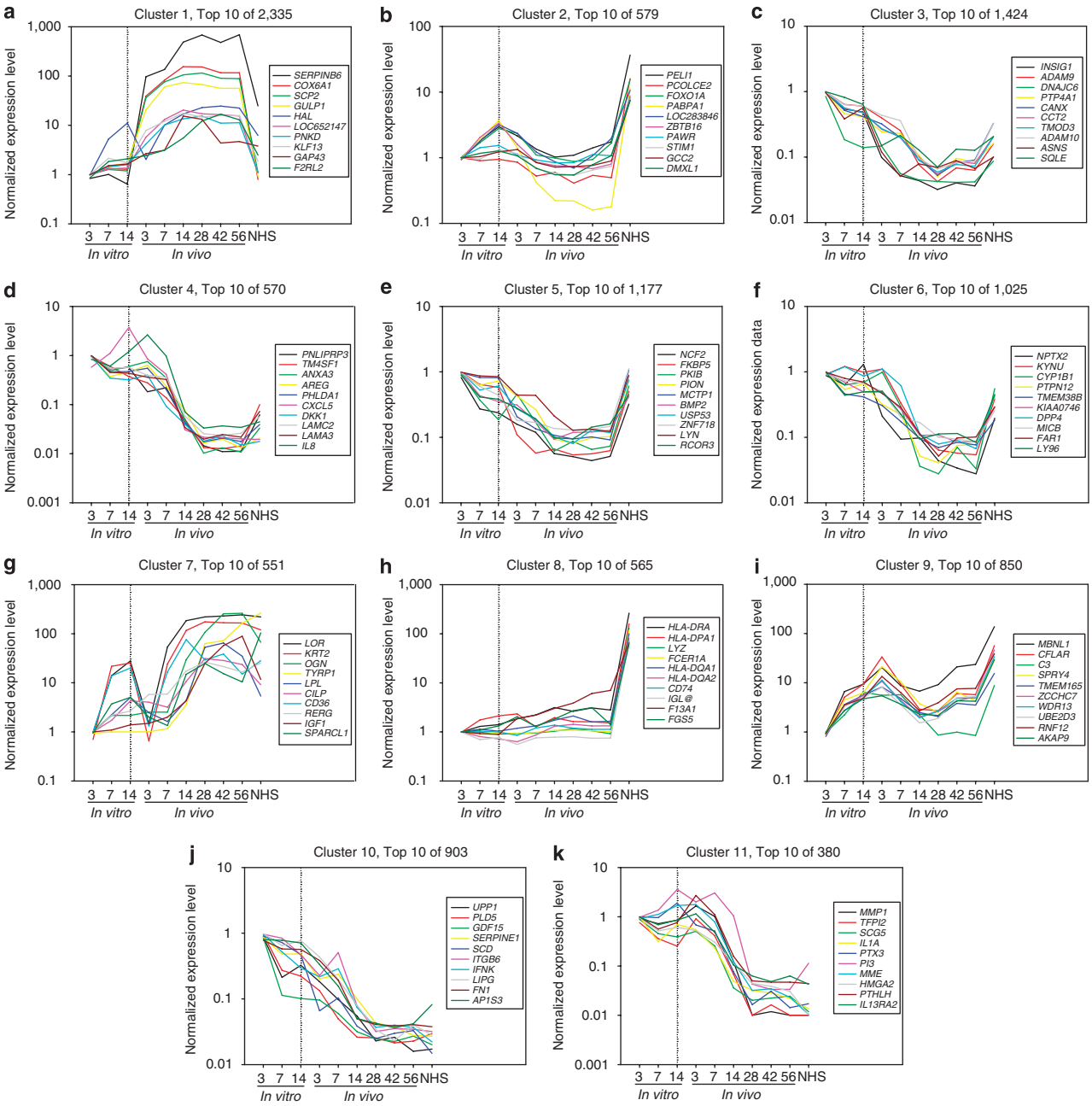

Figure 6. Expression of top 10 known genes of each cluster identified through hierarchical clustering. Expression levels were normalized to mean expression in CSS at day 3 *in vitro*. Mean normalized expression levels for genes in clusters 1–11 (**a**–**k**, respectively) plotted on the vertical axes *versus* sample types on the horizontal axes are shown. Note that the scales of the vertical axes vary between plots, but the horizontal axes are identical. Time of grafting to mice is indicated by a vertical dotted line on each plot.

and fetal development. Of the 24 different homeobox genes that were expressed in all 11 clusters, 17 were in cluster 1, including *HOXC4*, *HOXB5*, and *HOXB9*. Genes were ranked by the highest normalized expression at day 28 *in vivo*, and expression levels for the top 10 genes are shown in Figure 6a. The top-ranked gene in cluster 1 is *SERPINB6*, which was expressed at over 600-fold higher levels at day 28 *in vivo* compared with *in vitro* expression levels.

Cluster 2 contains 579 probe sets, representing 449 non-redundant genes, which were expressed at relatively high levels in NHS, but were expressed at low levels in CSS. Genes in this cluster were ranked by descending expression in NHS. Pathway analysis (Supplementary Table S2) revealed that genes involved in transcription, metabolism, and regulation of cellular processes were significantly associated with cluster 2. For example, top ranked genes in cluster 2 include *Pelino homolog 1* (*PELI1*), which is required for interleukin-1-mediated signaling (Jiang *et al.*, 2003); *procollagen C-endopeptidase enhancer 2* (*PCOLCE2*), which is involved in collagen biosynthesis; the forkhead transcription

factor *FOXO1A*; and *nuclear poly(A)-binding protein 1* (*PABPN1*), which is involved in addition of poly(A) tails to eukaryotic transcripts. These genes were more highly expressed in NHS compared with CSS; therefore, pathways involving these genes may be partially lacking in CSS *in vitro* and after grafting.

Cluster 3 contains 1,424 probe sets representing 1,214 nonredundant genes. These genes were expressed at relatively high levels *in vitro,* particularly at day 3, but were downregulated after grafting, dropping to relatively low or absent levels by days 14–28 *in vivo* and remaining lower in CSS than in NHS. Genes in this cluster were ranked on the basis of ascending expression in CSS at day 28 after grafting. Pathway analysis indicated a significant association of cluster 3 genes with processes involved in biosynthesis, including translation, protein folding, RNA processing, and NADH dehydrogenase activity, which are predicted to be important for cells with high mitotic rates (Supplementary Table S2). Consistent with this characterization, several of the top ranked genes in cluster 3 encode proteins associated with the endoplasmic reticulum, such as *insulin-induced gene 1* (*INSIG1*) and *protein tyrosine phosphatase type IVA member 1* (*PTP4A1*), or having molecular chaperone activity, such as *calnexin* (*CANX*), *DnaJ homolog subfamily C member 6* (*DNAJC6*), and *chaperonin-containing TCP1 subunit 2* (*CCT2*) (Figure 6c).

Cluster 4 contains 570 probe sets, representing 442 nonredundant genes, which were expressed *in vitro* and at early *in vivo* time points, but were downregulated by day 14 *in vivo* and were low or off in NHS. Pathway analysis identified cell proliferation, cell motility, apoptosis, and development/morphogenesis as important processes associated with genes in cluster 4. These pathways indicate processes that are required for epidermal stratification and healing of CSS after transplantation. The genes in cluster 4 were ranked by ascending expression levels in CSS at day 42 *in vivo* (Figure 6d). Several of the top ranked genes in cluster 4 are involved in inflammation, epidermal proliferation, and differentiation, including interleukin 8 and chemokine (C-X-C motif) ligand 5. These genes were expressed in CSS at day 14 *in vitro* and at day 3 *in vivo,* but were essentially undetectable at later time points *in vivo,* reflecting decreased inflammation and proliferation in CSS after healing. Furthermore, highly ranked in cluster 4 were *laminin gamma 2* (*LAMC2*) and *alpha 3* (*LAMA3*) genes, which encode 2 of the 3 subunits of laminin 5, a structural component of the epidermal basement membrane, suggesting that this structure is established during the early time points of CSS morphogenesis.

Cluster 5 contains 1,177 probe sets representing 974 nonredundant genes that were expressed *in vitro* but were downregulated after grafting, and were expressed at higher levels in NHS compared with healed CSS. Pathways, structures, and processes significantly associated with cluster 5 include protein metabolic processes, RNA binding, metabolism, protein localization, intracellular organelles, and cytoplasm (Supplementary Table S2). The expression profile and pathway analysis of cluster 5 show similarities with cluster 3, but with a relatively higher expression in NHS, which is similar to expression levels in CSS *in vitro*.

These genes were ranked by ascending expression levels in CSS at day 42 *in vivo* (Figure 6e). Highly ranked cluster 5 genes include *neutrophil cytosolic factor 2* (*NCF2*), which encodes a subunit of the multiprotein nicotinamide adenine dinucleotide phosphate oxidase, and *FK506-binding protein 5* (*FKBP5*), which forms part of a complex with the glucocorticoid receptor. Another top ranked gene was *bone morphogenetic protein 2* (*BMP2*), a growth factor related to transforming growth factor-β. *BMP2* expression was found in mouse skin to be localized to matrix cells of the hair follicle, coincident with terminal differentiation, suggesting a role in the termination of cell proliferation (Blessing *et al.*, 1993). Expression of bone morphogenetic protein 2 in NHS is approximately 3.5-fold higher than that in healed CSS *in vivo,* and may be associated with the presence of hair follicles in NHS.

Cluster 6 contains 1,025 probe sets and 862 nonredundant genes that were expressed at relatively higher levels in CSS *in vitro* and at day 3 after grafting, but were downregulated to very low levels by day 42 after grafting, slightly below the levels found in NHS. The expression profile of cluster 6 is similar to that of cluster 3, and pathway analysis indicates similar processes and components as well, including metabolism and organelles (Supplementary Table S2), although the genes were clustered from separate branches of the hierarchical tree (Figure 5). The genes in Cluster 6 were ranked by ascending expression levels in CSS at day 42 after grafting. Highly ranked genes in cluster 6 include *kynureninase* (*KYNU*), an enzyme involved in tryptophan metabolism; *cytochrome P450 family 1 subfamily B polypeptide 1* (*CYP1B1*), a member of the cytochrome P450 superfamily of enzymes; and *fatty acyl CoA reductase 1* (*FAR1*) (Figure 6f).

Cluster 7 contains 551 probe sets, representing 412 nonredundant genes that were highly expressed after grafting, particularly after 7 days *in vivo,* and which were generally expressed at high levels in NHS (Figure 6g). The fold changes in the expression of these genes from day 3 *in vitro* to day 56 *in vivo* were markedly higher than those seen in the other clusters of genes. Pathway analysis revealed that genes in cluster 7 are involved in development, including skeletal and lymphoid organ development, protein binding, cell adhesion, and extracellular matrix (Supplementary Table S2). Cluster 7 genes were ranked by descending order of expression at day 28 *in vivo*. The two highest ranked genes in cluster 7 were *LOR* and *KRT2,* which were also among the most highly induced genes *in vitro* (Figure 3), and showed the greatest expression decreases immediately after grafting (Figure 4a). *KRT2* and *LOR* were the most highly induced genes *in vivo,* increasing approximately 254-fold and 165-fold, respectively, between days 3 and 56 after grafting to mice (Figure 6g). Expression of these proteins in CSS after grafting suggests that keratinocytes in CSS display a differentiated epidermis similar to those in NHS.

Furthermore, the gene that is highly induced in CSS after grafting and is among the top ranked genes in cluster 7 is the melanocyte-specific gene *tyrosinase-related protein 1*

(*TYRP1*). Other melanocyte-specific genes found in cluster 7 include *dopachrome tautomerase* (*DCT*), *melan-A* (*MLANA*), and *silver* (*SILV*) (Table S1 online). Increased expression of these genes correlates with increased pigmentation of CSS after grafting by passenger melanocytes, as illustrated in Figure 2.

Cluster 8 contains 565 probe sets, representing 423 nonredundant genes, which were expressed at low or absent levels in CSS at all time points, but were highly expressed in NHS (Figure 6h). Pathways, cellular components, and functions of genes in cluster 8 included plasma membrane, major histocompatability class II protein complex, hemopoietic or lymphoid organ development, immune system development, and signal transducer activity, as well as cell adhesion, response to wounding, and positive regulation of mesenchymal cell proliferation (Supplementary Table S2). Cluster 8 genes were ranked by their highest expression in NHS. As illustrated by the identities of the top ranked genes in cluster 8 (Figure 6h), including multiple major histocompatability antigen genes, many cluster 8 genes are expressed in cell types that are absent from CSS *in vitro*, such as cells of the human immune system. In addition, endothelial cell-specific genes, including *platelet/endothelial cell adhesion molecule* (*PECAM1*), *endomucin* (*EMCN*), and *von Willebrand factor* (*VWF*), were present in cluster 8 (Supplementary Table S1), reflecting the presence of a vasculature in native skin and the absence of human endothelial cells in CSS *in vitro* and after grafting.

Cluster 9 contains 850 probe sets, or 627 nonredundant genes, which were increased in CSS during *in vitro* maturation, but downregulated after grafting to lower levels than those in NHS (Figure 6i). This expression pattern is similar to that of cluster 2, but the gene cluster was obtained from different branches of the hierarchical tree (Figure 5). Pathway analysis showed that genes involved in positive regulation of metabolic processes, negative regulation of cell-cycle progression, cell development, DNA-dependent transcription, and the ubiquitin cycle were significantly associated with cluster 9 (Supplementary Table S2). The genes in cluster 9 were ranked on the basis of their highest relative expression at day 14 *in vitro* (Figure 6i). The top ranked gene is *muscleblind 1* (*MBNL1*), a regulator of tissue-specific alternate pre-mRNA splicing (Ho *et al.*, 2004; Pascual *et al.*, 2006). Other highly ranked genes include *ubiquitin-conjugating enzyme E2D 3* (*UBE2D3*), a member of the E2 ubiquitin-conjugating enzyme family (Saville *et al.*, 2004), and *ring finger protein 12* (*RNF12*), a co-repressor of LIM homeodomain transcription factors with intrinsic ubiquitin ligase activity (Ostendorff *et al.*, 2000).

Cluster 10 contains 903 probe sets (787 nonredundant genes) that were expressed at relatively high levels *in vitro*, were downregulated after grafting, reaching negligible levels by day 56 *in vivo*, and were expressed at low levels in NHS (Figure 6j). The expression profile of cluster 10 genes is similar to that of cluster 3, but with lower or absent expression in NHS. Processes and cellular components significantly associated with Cluster 10 include biosynthesis, metabolic processes, organelle lumen, protein transporter activity, and mitochondrion (Supplementary Table S2). The genes in cluster 10 were ranked by the lowest expression levels at day 56 *in vivo*. Among the top ranked genes in this cluster are *integrin β-6* (*ITGB6*) and *serpin peptidase inhibitor clade E member 1* (*SERPINE1*), which were shown by others to be absent from normal skin but highly induced on wounding (Haapasalmi *et al.*, 1996; Hakkinen *et al.*, 2004). The expression of *ITGB6* and *SERPINE1* in CSS during *in vitro* maturation is consistent with a wound healing phenotype previously described for CSS *in vitro* (Smiley *et al.*, 2005a).

Cluster 11 contains 380 probe sets, or 303 nonredundant genes, which were expressed in CSS *in vitro* and were upregulated at early time points after grafting, but were downregulated within 4 weeks of grafting and were low or absent in NHS. Pathway analysis indicates a significant association of cluster 11 genes with cell motility and locomotory behavior, developmental processes, and response to chemical and external stimuli (Supplementary Table S2). These processes are characteristic of genes expressed in the early phases of wound healing.

Genes in this cluster were ranked by lowest expression at day 42 *in vivo*. The top ranked gene in cluster 11 is *matrix metalloproteinase 1* (*MMP1*), which was shown in a previous study to be expressed during cutaneous wound healing in which it is involved in matrix remodeling (Chen *et al.*, 2001). MMP1 was expressed at CSS *in vitro*, peaked at 3 days after grafting, and was essentially absent within 28 days of grafting (Figure 6k). Other wound healing-associated genes in cluster 11 included the *peptidase inhibitor 3* (*PI3*), which was relatively highly expressed in CSS at day 14 *in vitro* through to day 14 *in vivo*, and *parathyroid hormone-like protein* (*PTHLH*), which was highest in CSS at 3 days after grafting. Consistent with the wound healing nature of cluster 11, genes encoding keratin proteins characteristically expressed in activated keratinocytes were found in cluster 11 (*KRT6A*, *KRT6B*, *KRT16*, and *KRT17*; Supplementary Table S1). The expression of these keratins was highest in CSS at or immediately after grafting, and dropped to levels approaching NHS by later *in vivo* time points, consistent with previously published findings from our laboratory (Smiley *et al.*, 2005b).

Validation by immunohistochemistry

Immunohistochemistry showed that KRT2 and LOR proteins, both characteristic of differentiated keratinocytes of the cornified envelope, were co-expressed in an interesting pattern *in vitro* and *in vivo*. Both transcripts were among the transcripts most highly induced during *in vitro* incubation (Figure 3); the proteins were not detected in CSS at day 3 *in vitro* (data not shown), but were detectable in the suprabasal epidermis at day 14 *in vitro* (Figure 7a and b). At day 3 after grafting, KRT2 and LOR showed the highest fold decreases in RNA expression (Figure 4a), and the proteins were not detectable in CSS sections (Figure 7c and d). However, expression of both genes was increased by day 14 after grafting, and by day 56, the observed RNA levels and protein expression patterns were similar to those of

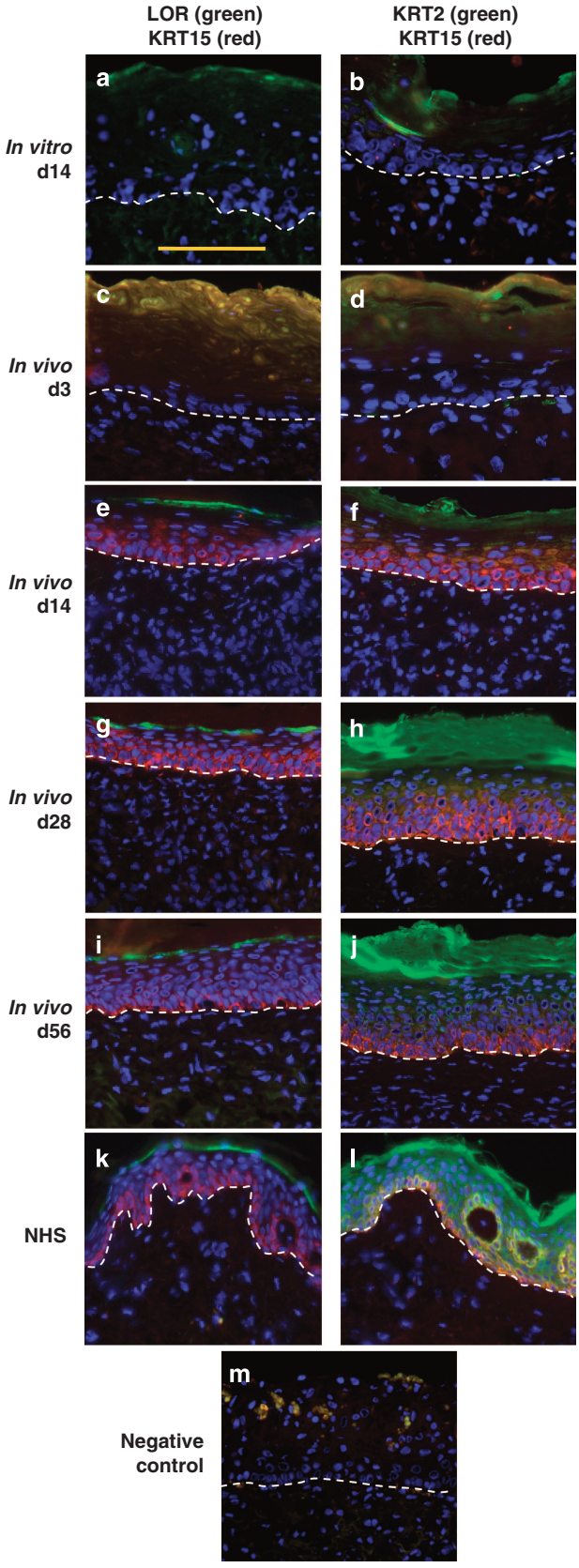

NHS (Figure 6g and Figure 7i–l). Previous studies from our laboratory showed an increased expression of the basal cell marker KRT15 after grafting CSS to mice (Smiley *et al.*, 2005b), and this was confirmed in this study. KRT15 expression was observed in ESS within 14 days of grafting, and localized basal cell expression was observed within 56 days of grafting, similar to NHS (Figure 7).

Immunohistochemistry was also used to evaluate the expression of three genes highly expressed in CSS, which were described previously to have roles in cartilage and bone development: *osteoglycin* (*OGN*), also known as *osteoinductive factor* or *mimecan*, *cartilage intermediate layer protein* (*CILP*), and *periostin* (*POSTN*), also known as *osteoblast-specific factor* (ranked 3, 6, and 280, respectively, in cluster 7). *CILP*, previously identified in cartilage and reported to be cartilage-specific (Lorenzo *et al.*, 1998), was expressed in the epidermal compartment of CSS after grafting at levels higher than those observed in NHS (Figure 8). *POSTN* and *OGN* have been reported previously by separate groups to be involved in the regulation of collagen fibrillogenesis (Tasheva *et al.*, 2002; Norris *et al.*, 2007). In particular, *POSTN* was suggested to regulate the viscoelastic properties of skin (Norris *et al.*, 2007). In this study, *POSTN* protein was localized to the upper dermis of CSS *in vivo*, particularly at day 56 *in vivo*, and also to NHS (Figure 8). The *POSTN* expression in CSS seems more widespread than that of NHS, which could reflect differences in elasticity between CSS grafted to mice and NHS. Interestingly, immunohistochemistry localized *OGN* primarily to the epidermis of CSS *in vivo* (Figure 8).

Network analysis of adhesion-related genes

As a number of related biological processes were present in the different gene set enrichments of the 11 clusters, cytoscape-enabled network analysis was used to gain further insight into their connectivity (Shannon *et al.*, 2003). Biological adhesion was highly enriched in multiple clusters; we therefore connected the sets of genes from each cluster that were associated with shared categories of adhesion-related processes. As illustrated in Figure 9, 149 of the genes from six clusters were involved in cell adhesion. However, as they were differentially regulated across the different clusters, the emerging suggestion from this network is that the regulation and execution of cell–cell and cell–extracellular matrix adhesion are accomplished by different specific genes that are activated or repressed at various times in the course of engineered skin morphogenesis (Figure 9). For example, genes involved in cell–cell adhesion, cell–matrix adhesion,

Figure 7. Expression of basal keratinocyte and cornified envelope proteins is similar in healed CSS and NHS. Immunohistochemistry (**a**–**j**) using antibodies specific for KRT15 (red fluorescence; **a**–**l**), LOR (green fluorescence; **a**, **c**, **e**, **g**, **i**, **k**), and KRT2 (green fluorescence; **b**, **d**, **f**, **h**, **j**, **l**) showing expression in CSS (**a**–**j**) and NHS (**k** and **l**), as indicated. For the negative control section of CSS (**m**), primary antibodies were omitted but both secondary antibodies were used. Dotted white lines indicate locations of dermal–epidermal junctions. All sections were counterstained with 4′,6 diamidino-2-phenylindole, which stains nuclei blue. Scale bar in panel (**a**) is the same for all sections, 0.1 mm.

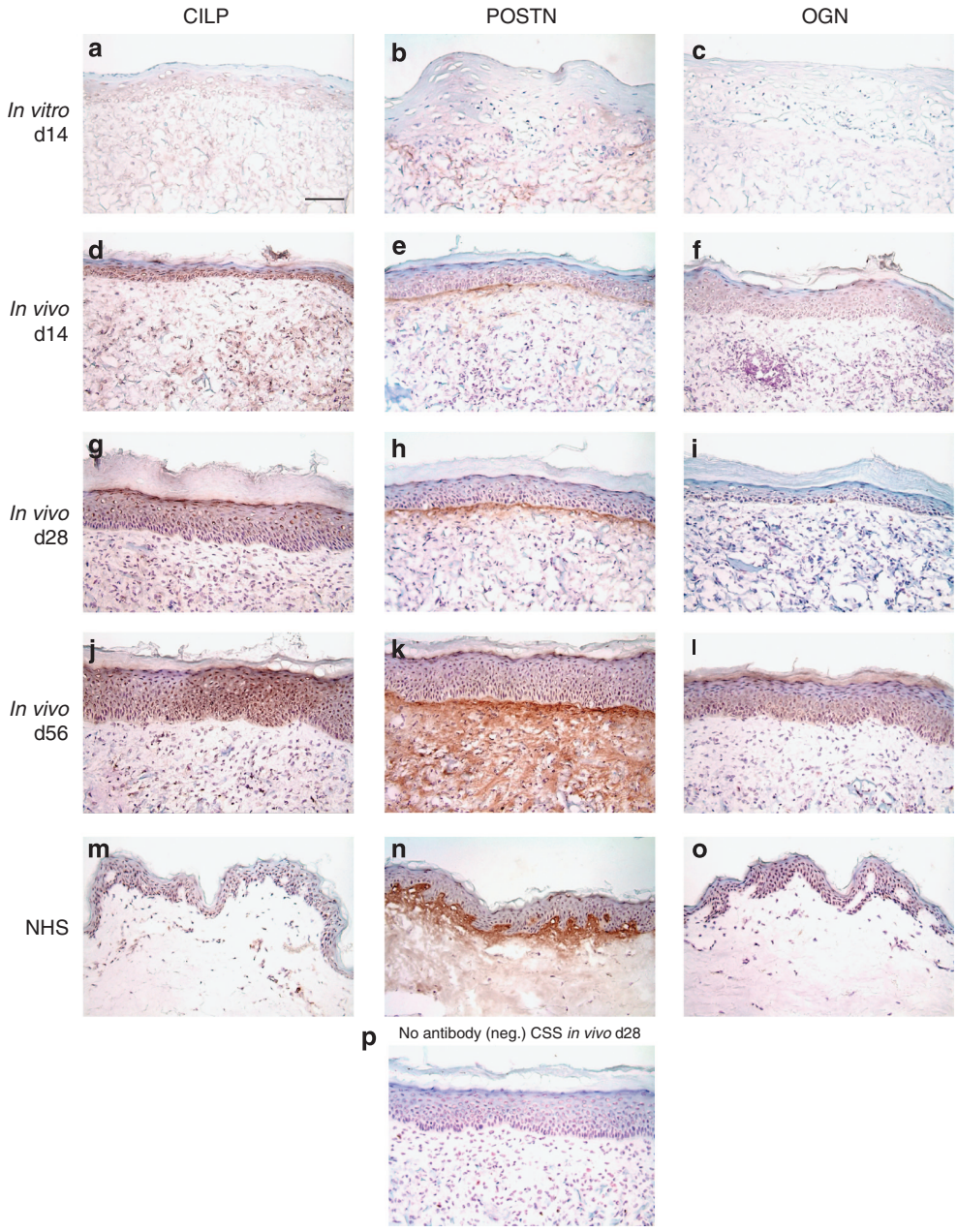

Figure 8. Expression of proteins involved in cartilage and bone biology in engineered and native skin. Immunohistochemistry using antibodies specific for CILP (**a**, **d**, **g**, **j**, **m**), POSTN (**b**, **e**, **h**, **k**, **n**), and OGN (**c**, **f**, **i**, **l**, **o**), showing expression in CSS (**a**–**l**) and NHS (**m**–**o**), as indicated. Negative control immunostaining was carried out with primary antibody omitted (**p**). Scale bar in panel (**a**) is the same for all sections, 0.1 mm.

and focal adhesion were enriched in cluster 4, as were genes involved in keratinocyte differentiation (Figure 9). Among these genes were *integrin* β-*4* (*INTB4*) and *integrin alpha 6* (*INTA6*), which were induced in CSS *in vitro* and were elevated through 1 week after grafting, consistent with the period of establishment of cell–cell contacts, keratinocyte differentiation, and inflammation. *INTB4* and *INTA6* were linked through common network associations to a gene set previously published by Passerini *et al.* 2004 and to four additional published studies (Santoro *et al.*, 2003; Yebra *et al.*, 2003; Enserink *et al.*, 2004; Turner *et al.*, 2006), which increase our understanding of the roles of these genes in epithelial adhesion (Figure 9). Taken together, this network-based global genomic analysis suggests that diverse groups of adhesion genes work together through a stepwise assembly to form a complex tissue structure necessary to fulfill the critical integrity, adhesion, and flexibility necessary for skin function.

DISCUSSION

This report describes, to our knowledge, the first reported comprehensive analysis of gene expression dynamics that underlie the successful establishment of engineered skin

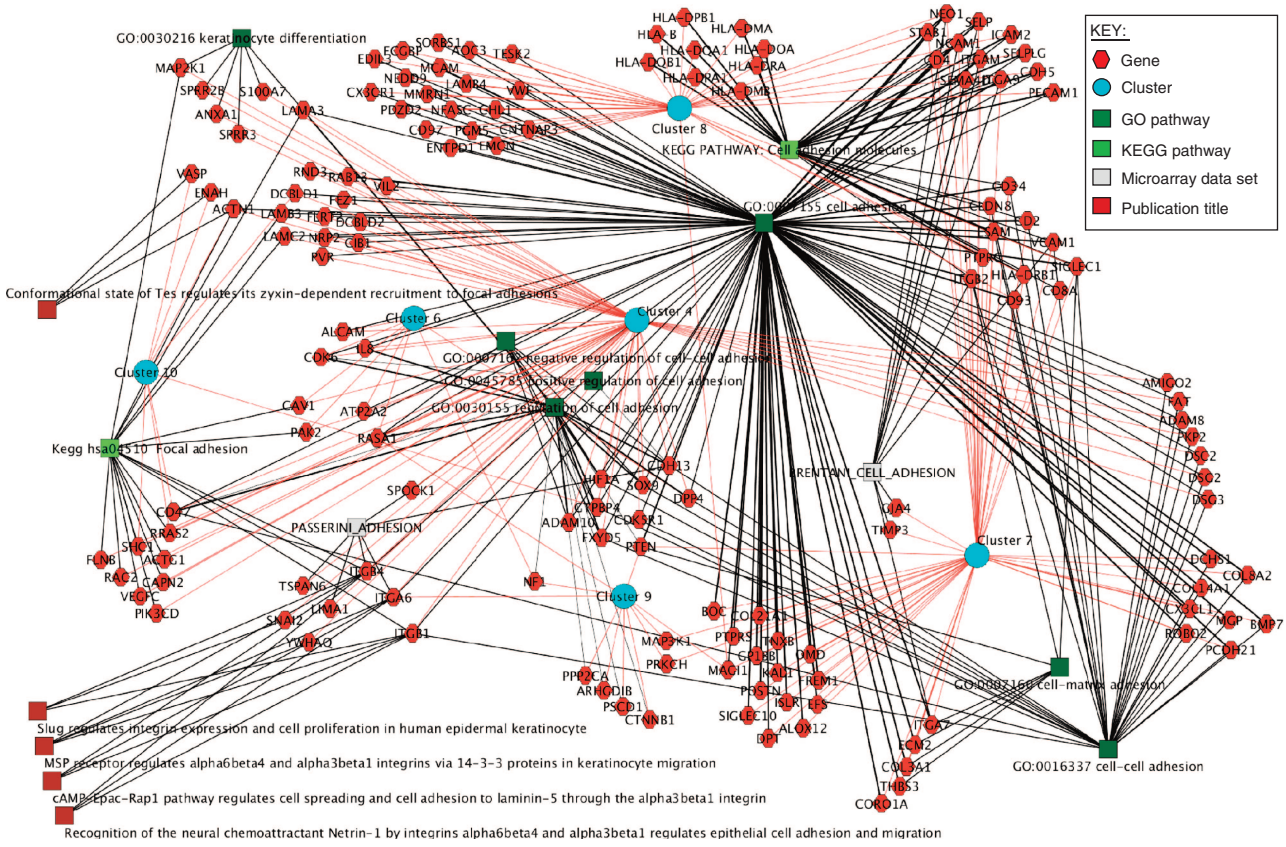

Figure 9. Adhesion pathway gene association network. Network analysis showing adhesion-related genes expressed in cultured skin substitutes and associated Gene Ontology (GO) pathways, KEGG pathways, overlapping published microarray data sets (Brentani *et al.*, 2003; Passerini *et al.*, 2004), and PubMed articles (Garvalov *et al.*, 2003; Santoro *et al.*, 2003; Yebra *et al.*, 2003; Enserink *et al.*, 2004; Turner *et al.*, 2006) among corresponding gene clusters, obtained using Cytoscape bioinformatics software (Shannon *et al.*, 2003). This analysis shows that adhesion pathway genes are highly enriched in multiple clusters, indicating that different expression behaviors act in concert to regulate the different types of adhesive properties required for morphogenesis and *in vivo* adaptation of engineered human skin.

in vitro and *in vivo* after orthotopic transplantation. Similar analyses have been reported for engineered oral mucosa (Alaminos *et al.*, 2007) and kidney (Rosines *et al.*, 2007), but these studies were limited to characterization of *in vitro* tissue-engineered substitutes and comparison with native tissue. Our laboratory previously reported the expression profile of *in vitro*-matured CSS compared with gene expression in fibroblasts, keratinocytes, and native skin (Smiley *et al.*, 2005a). We hereby extend these findings to examine gene expression during the *in vitro* development of CSS and at multiple time points after grafting to full-thickness wounds in mice. By linking pathway analyses with hierarchical clustering of gene expression patterns, we can now appreciate critical molecular events and details that enable engineered skin morphogenesis *in vitro* and, importantly, during adaptation *in vivo*.

Within 3 days of combining keratinocytes with fibroblasts in the biopolymer matrix, genes involved in biosynthetic pathways were found to be significantly upregulated. These include genes that regulate RNA processing, protein folding, biopolymer modification and metabolism, intracellular transport, and translation. For example, genes highly expressed *in vitro* and downregulated after grafting (cluster 3) include *INSIG1*, an endoplasmic reticulum protein that has an important role in cholesterol homeostasis (Yang *et al.*, 2002), and *PTP4A1* that was shown to be localized to the endoplasmic reticulum and mitotic spindle, and to be involved in the regulation of cell proliferation and transformation (Wang *et al.*, 2002). Thus, the cells in CSS *in vitro* are rapidly dividing and synthesizing proteins required for organization of a multilayer tissue.

Members of the ADAM (a disintegrin and metalloprotease) family, *ADAM9* and *ADAM10*, were expressed at relatively high levels *in vitro* and dropped to negligible levels after grafting; these genes are two of the top ranked genes in cluster 3. *ADAM* genes encode transmembrane proteases implicated in the release of bound factors and peptides, such as the ectodomains of membrane-bound proteins. ADAM9 has been shown to interact with the β1 integrin subunit on keratinocytes and regulate cell migration (Zigrino *et al.*, 2007), and ADAM10 regulates the shedding of E-cadherin and localization of β-catenin in HaCaT keratinocytes (Maretzky *et al.*, 2005). Both ADAM9 and ADAM10 are implicated in the control of keratinocyte migration (Maretzky *et al.*, 2005; Zigrino *et al.*, 2007). Their relatively high expression in CSS at early *in vitro* time points suggests that

adhesion and cell migration are important functions during early CSS morphogenesis.

By the end of the *in vitro* time course, the predominant functions include biopolymer modification, protein binding, cell development, positive regulation of metabolism, and negative regulation of cell-cycle progression. Genes expressed in differentiated keratinocytes were among the most highly induced genes during the *in vitro* maturation of CSS, consistent with previous observations of the development of a partially functional epidermal barrier before grafting (Boyce *et al.*, 2002). Several of the genes that were highly induced in CSS *in vitro* (*S100A12*, *S100A7L1*, *LOR*, and *SPRR2C*) map to the EDC, a region of human chromosome 1 with a high density of genes involved in epidermal maturation (Marenholz *et al.*, 2001). Coordinately increased expression of these genes during *in vitro* incubation of CSS, combined with pathways analysis, indicates that component cells are still actively remodeling the matrix and continue to have high metabolic rates, but that differentiation processes are beginning to replace proliferative processes.

Marked changes in expression were observed after grafting CSS to mice. Very large fold changes were observed within 3 days of grafting, a period that corresponds to the initiation of angiogenesis from the host wound bed (Supp *et al.*, 2000); therefore, the wound environment exerted a strong influence on the physiology of engineered skin grafts, even before vascularization is achieved. *KRT2* and *LOR* were among the most highly induced genes *in vitro*, and interestingly, were also among the most highly downregulated 3 days after grafting. The downregulation of differentiation-specific genes may result in part from occlusion of the engineered skin graft after transplantation, which may have disrupted the barrier function while grafts were protected by dressing materials. The expression of *KRT2* and *LOR* increased after grafting to levels similar to those of native skin, suggesting the restoration of barrier function after healing of CSS. Another gene that was markedly decreased after grafting was *DEFB4*, which encodes human β-defensin 2, a peptide with broad-spectrum antimicrobial activity, which is induced in keratinocytes on differentiation (Liu *et al.*, 2002) and is also highly expressed in psoriatic epidermis (de Jongh *et al.*, 2005). In contrast to *KRT2* and *LOR*, expression of *DEFB4* was essentially undetectable at all time points after grafting. CSS are highly susceptible to microbial contamination after grafting, which has been attributed to the absence of a vascular plexus at the time of transplantation (Boyce *et al.*, 1995). Hypothetically, resistance to infection might be improved if elevated expression levels of DEFB4 were maintained after grafting.

In addition to these changes, genes expressed in basal keratinocytes of native skin, including *LGALS1*, *KRT15*, and *WNK lysine-deficient protein kinase 1* (*WNK1*), were induced in CSS after grafting. *LGALS1* encodes galectin-1, a multifunctional lectin that was shown to influence cell growth and apoptosis (Hsu and Liu, 2004). In skin, galectin-1 was reportedly expressed in basal epidermal cells and in undifferentiated keratinocytes originating from hair follicles, and was proposed as a marker of epidermal stem cells (Dvorankova *et al.*, 2005; Klima *et al.*, 2005). *KRT15* is also considered to be a stem cell marker (Webb *et al.*, 2004). *WNK1* serine–threonine kinase has been proposed to function in the regulation of electrolyte homeostasis and its expression was demonstrated in basal epidermal cells (Choate *et al.*, 2003); *WNK1* was expressed in CSS *in vitro* but was increased sixfold after graft healing. Another putative stem cell marker induced in CSS on grafting was *FHL1*, which was reported to be highly expressed in label-retaining stem cells of the epidermis (Tumbar *et al.*, 2004) and was shown to suppress keratinocyte differentiation (Grossi *et al.*, 2005). Previous studies from our laboratory showed that the KRT15 protein was absent from CSS *in vitro* (Smiley *et al.*, 2005b) and, further, that the proliferative population of cells in the basal epidermis of CSS significantly decreased with extended periods in culture (Boyce *et al.*, 2002). These results suggested that the basal stem cell population required for renewal of differentiating epidermal cells was depleted over time in culture. In pediatric burn patients, however, CSS have been shown to provide permanent wound closure and to grow in area as the patient grows (Boyce *et al.*, 2006), suggesting the presence of an epidermal stem cell compartment in CSS after grafting. The current gene expression data provide molecular evidence supporting the reestablishment of an epidermal stem cell compartment in CSS in response to factors that are present in the host after transplantation. Histological sections of grafts at 3 days *in vivo* showed a very thin epidermis, suggesting that there must still have been a minimum number of proliferative cells present that were capable of establishing an epidermal stem cell layer after transplantation.

In the early time period after grafting, genes associated with response to external stimuli, locomotion and cell motility, and response to stress are significantly upregulated, consistent with a wound healing phenotype. For example, *interleukin 8* (*IL8*) and *chemokine* (*C-X-C motif*) *ligand 5* (*CXCL5*) were highly ranked in cluster 4; they were expressed *in vitro* and at early *in vivo* time points, but were downregulated within 14 days of grafting. *IL8* is an inflammatory mediator expressed in suprabasal keratinocytes, which has been postulated to regulate epidermal stratification and wound healing (Konstantinova *et al.*, 1996). *IL8* was shown to be produced concomitantly with proinflammatory cytokine *CXCL5*, also ranked in the top 10 genes of cluster 4, in response to interleukin 1 signaling (Bersinger *et al.*, 2008).

Genes that regulate developmental processes and anatomical structure morphogenesis were highly expressed after grafting of CSS, as were the genes involved in apoptosis and programmed cell death, suggesting that tissue maturation, remodeling, and development occur after transplantation of CSS and during the healing process. Representation of developmental pathway genes increases at later time points; pathway analysis revealed a significant association with processes including skeletal development, hematopoietic development, and heart contraction, in clusters of genes expressed in CSS at later time points. The expression of selected genes implicated in skeletal development was

confirmed by immunohistochemistry. Rather than suggesting that the CSS adopt a skeletal or cardiac phenotype during healing, these results likely indicate that specific groups of genes are responsible for the regulation of multiple developmental events in divergent tissues.

Structural genes expressed in differentiated keratinocytes and proteins involved in the epidermal barrier were among the most highly induced in CSS during the *in vivo* time course. Many of these genes were similarly expressed in CSS and NHS, suggesting the development of a mature barrier function in CSS. Epidermal barrier is the definitive property of any skin graft, and this finding confirms that healed CSS provide wound coverage with similar barrier properties to native skin.

The microarray analysis, however, revealed marked differences in gene expression between healed CSS and NHS, providing insight into the limitations of engineered tissue. Some of these disparities are because of the absence of specific cell types in CSS. For example, genes involved in immune system development and MHC class II protein complexes were essentially absent from CSS at all time points examined, but were expressed at relatively high levels in NHS. In addition, genes linked with hair follicle development, such as *bone morphogenetic protein 2*, were expressed at higher levels in NHS compared with CSS. This differential expression may be because of the absence of hair follicles in CSS. Although hair follicles are absent from CSS, endothelial cells derived from host vasculature are known to be present (Supp *et al.*, 2000); however, because these cells are of mouse origin, no endothelial cell-specific genes were detected using human gene chips. It is expected that hybridization of the same CSS RNA samples to mouse gene chips would reveal the expression of endothelial-specific genes such as vWF and CD31.

Genes expressed in adherens junctions and tight junctions were expressed at significantly lower levels in CSS compared with NHS, suggesting the incomplete development of these structures in CSS through 8 weeks after grafting. Other processes were represented at early *in vivo* time points, but were downregulated to levels significantly lower than NHS after healing; these include posttranslational protein modification, transcription, and nucleic acid binding. These observations suggest that deficiencies in CSS remain, and may be used to guide future improvements to the model.

Identification of global gene expression profiles using microarray analysis can yield a wealth of information, and the current data set may serve as an atlas of gene expression for skin and skin tissue engineering. The gene expression data available in public databases can be further mined and evaluated to reveal new relationships with previously identified or newly discovered expression data. Analysis of interactions involving specific pathways provides insight into gene regulatory networks, which can be used to guide future developments in tissue engineering. As an example of the power of this analysis, genes involved in adhesion were subjected to network analysis to identify relationships between expression behaviors, expression data sets, and functional pathways. Taken together, our results indicate that there is a tremendous degree of enrichment of unifying biological themes related to adhesion and cell–cell interaction occurring across multiple expression pattern clusters. Thus, accompanying the processes of keratinocyte–fibroblast interaction, *in vitro* differentiation, and posttransplantation cellular stratification, multiple gene regulatory and differentiation programs exhibit sequential activation and repression of a wide variety of genes, which in turn are involved in regulating and accomplishing different aspects of cell–cell and cell–matrix adhesion.

MATERIALS AND METHODS

Preparation and grafting of CSS

Biopsy samples of normal human skin ($n=2$) were obtained, with the approval of the University of Cincinnati Institutional Review Board and according to the Declaration of Helsinki Principles, from breast tissue of healthy adult Caucasian females. Informed consent was not required because the skin was obtained from discarded surgical tissues. Biopsy samples of skin were used for RNA purification, preparation of histological sections, and establishment of primary cell cultures. Fibroblasts and keratinocytes were isolated, cultured separately in a specific growth medium (Boyce, 1998), and colleted for preparation of CSS at passage 2. CSS (starting area approximately 80 cm^2 each) were prepared using cells from two independent donors as described in detail elsewhere (Smiley *et al.*, 2005a). Briefly, fibroblasts grown to near confluence were collected and inoculated onto collagen–glycosaminoglycan polymer substrates at a density of 5×10^5 fibroblasts per cm^2. One day later, keratinocytes were collected at subconfluence (85–90%) and inoculated onto dermal substrates at a density of 1×10^6 keratinocytes per cm^2. CSS were cultured at the air–liquid interface for 2 weeks *in vitro*. Biopsy samples of CSS were collected during the *in vitro* culture period at days 3, 7, and 14 for RNA isolation, histological examination, and immunohistochemistry.

Animal studies were carried out with the approval of the University of Cincinnati Institutional Animal Care and Use Committee. CSS were cut into 2×2 cm^2 sections and were grafted to full-thickness excisional wounds on the right flanks of 24 athymic nu/nu mice (Boyce, 1998). Mice were killed at 3, 7, 14, 28, 42, or 56 days after grafting ($n=4$ per time point, including at least one from each original skin donor). Biopsy samples were collected for preparation of RNA, and for histology and immunohistochemistry. Biopsy samples for RNA were obtained from the centers of grafted areas and did not contain mouse skin from the wound border. To confirm engraftment, human keratinocytes in grafted CSS were identified by immunohistochemistry using a fluorescein-labeled anti-human HLA-ABC antibody (Ab) (Accurate Chemical and Scientific., Westbury, NY). Samples without a positive signal were not analyzed further (data not shown).

Microarray analysis

Biopsy samples of normal adult female breast skin, or from CSS *in vitro* or CSS *in vivo*, were used for the preparation of total RNA using the RNeasy Mini Kit (QIAGEN, Valencia, CA), followed by further purification using phenol and chloroform extraction, and ethanol precipitation. RNA quality was analyzed using the Agilent Bioanalyzation system (Agilent Technologies, Palo Alto, CA) to ensure the integrity of RNA. A total of three samples per time point, representing the highest quality RNA preparations, and at least one

sample from each skin donor, were selected; owing to RNA degradation, only two samples were available for the day 3 *in vitro* and day 56 *in vivo* time points. Complementary DNA synthesis and hybridization to the Affymetrix Human U133 Plus 2.0 gene chip (Affymetrix, Santa Clara, CA) were performed by the Affymetrix Gene Chip Core Facility at Cincinnati Children's Hospital Medical Center (Cincinnati, OH) using standard protocols.

The hybridized arrays were scanned using Microarray Suite (MAS) Software (Affymetrix) and were analyzed with GeneSpring Software (Silicon Genetics, Redwood City, CA). To identify differentially expressed genes for each time point, an initial analysis of variance using Student's *t*-test, with a false discovery rate cutoff of 0.05 using the Benjamini–Hochberg test, was used. The values for RNA expression were converted into relative levels by referencing the expression value data to the mean expression values of the *in vitro* day 3 CSS. The analysis was focused on genes highly expressed in NHS, in CSS *in vitro*, or in CSS *in vivo*. A list of 10,359 probe sets was subjected to hierarchical clustering to obtain 11 clusters of genes representing different expression profiles that varied by sample type and time. During the analysis of individual probe sets and genes, care was taken to exclude loci that corresponded to sequences removed from public databases, and to disregard results that may have been because of artifact (for example, mouse genes present on the human gene chip). The entire data set is available online at http://www.ncbi.nlm.nih.gov/geo/ (accession #GSE17539).

To assess the relative gene-associated functions that were enriched in each different expression pattern cluster, we undertook a comparative cluster enrichment approach using a modified version of Gene Set Enrichment Analysis. Each list of genes from the 11 different clusters was separately examined for relative enrichment of genes that are associated with gene ontology, pathways, and transcription factor binding sites, as derived from analyses performed using the MSigDB (http://www.broad.mit.edu/gsea/msigdb/) reference database (Subramanian *et al.*, 2005). The enrichment *P*-value was converted into an intensity score by using the formula $S = (-\log(P\text{-value}))$. Specifically, for transcription factor binding sites, we mined the catalog of human-, mouse-, rat-, and dog-conserved regulatory motifs in promoters (4 kb; Xie *et al.*, 2005), using ToppGene server (Chen *et al.*, 2009), for each K-means-generated gene list. For preparation of Supplementary Table S2, biological processes, molecular functions, and cellular components for each cluster were ranked by the most significant *P*-value. Highly similar categories that had identical sets of genes (for example, ''cell death'' and ''death'') were only listed once. Up to six genes per category were randomly selected for inclusion in Supplementary Table S2; these genes were chosen from the list of genes for each cluster that were secondarily ranked by maximal fold change dysregulation. Note that these do not represent genes showing the highest expression levels.

To obtain network views of highly enriched Gene Ontology, Pathways, and PubMed articles among the corresponding gene clusters, we used Cytoscape (Shannon *et al.*, 2003), a JAVA-based bioinformatics software package for visualizing, modeling, and analyzing molecular and genetic interaction networks. Cytoscape provides a unique *in silico* approach to examine and display gene association networks on the basis of shared associations from either previous studies or computational predictions (Ideker *et al.*, 2002; Shannon *et al.*, 2003; Spirin and Mirny, 2003). The results from each gene selection method described above were entered as a matrix of data using the ToppGene server (Chen *et al.*, 2009).

Immunohistochemistry

Biopsy samples of NHS and CSS were embedded in a frozen state using M1 embedding matrix (Lipshaw, Pittsburgh, PA). Fluorescent immunostaining was performed using the following Abs: rabbit anti-mouse/human loricrin (Covance, Emeryville, CA), followed by fluorescein-conjugated goat anti-rabbit IgG (Santa Cruz Biotechnology, Santa Cruz, CA); rabbit anti-keratin 2 (Aviva Systems Biology, San Diego, CA), followed by fluorescein-conjugated goat anti-rabbit IgG (Santa Cruz Biotechnology); and chicken anti-keratin 15 (Covance), followed by Texas-Red-conjugated goat anti-chicken Ab (Abcam, Cambridge, MA). Sections were incubated with primary and secondary Abs for 1 hour at room temperature in a humidified chamber. Counterstaining was carried out using Vectashield mounting media containing 4′,6 diamidino-2-phenylindole for coverslipping (Vector Laboratories, Burlingame, CA). Colorimetric immunohistochemistry was carried out using the following primary Abs: goat anti-cartilage intermediate layer protein (Abcam); goat anti-ostoeglycin; and goat anti-periostin (both purchased from Santa Cruz Biotechnology). Ab detection used the Vectastain Elite ABC Kit (goat IgG) with 3,3-diaminodbenzidine substrate (Vector Laboratories), and sections were counterstained using hematoxylin QS (Vector Laboratories). For negative controls, serial sections were incubated in parallel without primary Ab. Sections were examined using a Microphot-FXA microscope (Nikon, Melville, NY) and were photographed using a Spot-Jr. Digital Camera (Diagnostic Instruments, Sterling Heights, MI).

CONFLICT OF INTEREST

The authors state no conflict of interest.

ACKNOWLEDGMENTS

The authors are grateful to the staff of Shriners Burns Hospital Engineered Skin Laboratory, including Jodi Miller, Christopher Lloyd, Rachel Zimmerman, Jill Pruszka, and John Besse for preparation of reagents required for CSS fabrication; to Deanna Leslie of the Shriners Burns Hospital Histology Core Facility for preparation of tissue sections; and to Dr John Kitzmiller of the Department of Surgery at the University of Cincinnati for providing human skin samples. At Cincinnati Children's Hospital Medical Center, we thank Shawn Smith and the staff of the Gene Expression Microarray Core, and Bhuvana Sakthivel in the Division of Biomedical Informatics, for their expert assistance. This study was funded by Medical Research Grants #8680 and #8450 from Shriners Hospitals for Children. Bioinformatics was supported in part by NIH P30DK078392-01.

SUPPLEMENTARY MATERIAL

Supplementary material is linked to the online version of the paper at http://www.nature.com/jid

REFERENCES

Alaminos M, Garzon I, Sanchez-Quevedo MC, Moreu G, Gonzalez-Andrades M, Fernandez-Montoya A *et al.* (2007) Time-course study of histological and genetic patterns of differentiation in human engineered oral mucosa. *J Tissue Eng Regen Med* 1:350–9

Barai ND, Supp AP, Kasting GB, Visscher MO, Boyce ST (2007) Improvement of epidermal barrier properties in cultured skin substitutes after grafting onto athymic mice. *Skin Pharmacol Physiol* 20:21–8

Bersinger NA, Frischknecht F, Taylor RN, Mueller MD (2008) Basal and cytokine-stimulated production of epithelial neutrophil-activating

peptide-78 (ENA-78) and interleukin-8 (IL-8) by cultured human endometrial epithelial and stromal cells. *Fertil Steril* 89:1530–6

Blessing M, Nanney LB, King LE, Jones CM, Hogan BL (1993) Transgenic mice as a model to study the role of TGF-beta-related molecules in hair follicles. *Genes Dev* 7:204–15

Boyce ST (1998) Methods for serum-free culture of keratinocytes and transplantation of collagen-GAG based composite grafts. In: *Methods in Tissue Engineering*. (Morgan JR and Yarmush M, eds). Totowa, NJ: Humana Press, 365–89

Boyce ST, Kagan RJ, Greenhalgh DG, Warner P, Yakuboff KP, Palmieri T *et al.* (2006) Cultured skin substitutes reduce requirements for harvesting of skin autograft for closure of excised, full-thickness burns. *J Trauma* 60:821–9

Boyce ST, Supp AP, Harriger MD, Greenhalgh DG, Warden GD (1995) Topical nutrients promote engraftment and inhibit wound contraction of cultured skin substitutes in athymic mice. *J Invest Dermatol* 104:345–9

Boyce ST, Supp AP, Swope VB, Warden GD (2002) Vitamin C regulates keratinocyte viability, epidermal barrier, and basement membrane formation *in vitro*, and reduces wound contraction after grafting of cultured skin substitutes. *J Invest Dermatol* 118:565–72

Brentani H, Caballero OL, Camargo AA, da Silva AM, da SW Jr, Dias NE *et al.* (2003) The generation and utilization of a cancer-oriented representation of the human transcriptome by using expressed sequence tags. *Proc Natl Acad Sci USA* 100:13418–23

Chen CC, Mo FE, Lau LF (2001) The angiogenic factor Cyr61 activates a genetic program for wound healing in human skin fibroblasts. *J Biol Chem* 276:47329–37

Chen J, Bardes EE, Aronow BJ, Jegga AG (2009) ToppGene Suite for gene list enrichment analysis and candidate gene prioritization. *Nuc Acids Res* 37:W305–11

Choate KA, Kahle KT, Wilson FH, Nelson-Williams C, Lifton RP (2003) WNK1, a kinase mutated in inherited hypertension with hyperkalemia, localizes to diverse Cl-transporting epithelia. *Proc Natl Acad Sci USA* 100:663–8

de Jongh GJ, Zeeuwen PL, Kucharekova M, Pfundt R, van d V, Blokx W *et al.* (2005) High expression levels of keratinocyte antimicrobial proteins in psoriasis compared with atopic dermatitis. *J Invest Dermatol* 125:1163–73

Dvorankova B, Smetana K Jr, Chovanec M, Lacina L, Stork J, Plzakova Z *et al.* (2005) Transient expression of keratin 19 is induced in originally negative interfollicular epidermal cells by adhesion of suspended cells. *Int J Mol Med* 16:525–31

Enserink JM, Price LS, Methi T, Mahic M, Sonnenberg A, Bos JL *et al.* (2004) The cAMP-Epac-Rap1 pathway regulates cell spreading and cell adhesion to laminin-5 through the alpha3beta1 integrin but not the alpha6beta4 integrin. *J Biol Chem* 279:44889–96

Garner WL (1998) Epidermal regulation of dermal fibroblast activity. *Plast Reconstr Surg* 102:135–9

Garvalov BK, Higgins TE, Sutherland JD, Zettl M, Scaplehorn N, Kocher T *et al.* (2003) The conformational state of Tes regulates its zyxin-dependent recruitment to focal adhesions. *J Cell Biol* 161:33–9

Grossi M, Hiou-Feige A, Tommasi DV, Calautti E, Ostano P, Lee S *et al.* (2005) Negative control of keratinocyte differentiation by Rho/CRIK signaling coupled with up-regulation of KyoT1/2 (FHL1) expression. *Proc Natl Acad Sci USA* 102:11313–8

Haapasalmi K, Zhang K, Tonnesen M, Olerud J, Sheppard D, Salo T *et al.* (1996) Keratinocytes in human wounds express alpha v beta 6 integrin. *J Invest Dermatol* 106:42–8

Hakkinen L, Koivisto L, Gardner H, Saarialho-Kere U, Carroll JM, Lakso M *et al.* (2004) Increased expression of beta6-integrin in skin leads to spontaneous development of chronic wounds. *Am J Pathol* 164:229–42

Hammond NL, Jahoda CA (2008) Id2, Id3, and Id4 proteins show dynamic changes in expression during vibrissae follicle development. *Dev Dyn* 237:1653–61

Ho TH, Charlet B, Poulos MG, Singh G, Swanson MS, Cooper TA (2004) Muscleblind proteins regulate alternative splicing. *EMBO J* 23:3103–12

Hsu DK, Liu FT (2004) Regulation of cellular homeostasis by galectins. *Glycoconj J* 19:507–15

Ideker T, Ozier O, Schwikowski B, Siegel AF (2002) Discovering regulatory and signalling circuits in molecular interaction networks. *Bioinformatics* 18(Suppl 1):S233–40

Jiang Z, Johnson HJ, Nie H, Qin J, Bird TA, Li X (2003) Pellino 1 is required for interleukin-1 (IL-1)-mediated signaling through its interaction with the IL-1 receptor-associated kinase 4 (IRAK4)-IRAK-tumor necrosis factor receptor-associated factor 6 (TRAF6) complex. *J Biol Chem* 278: 10952–6

Klima J, Smetana K Jr, Motlik J, Plzakova Z, Liu FT, Stork J *et al.* (2005) Comparative phenotypic characterization of keratinocytes originating from hair follicles. *J Mol Histol* 36:89–96

Konstantinova NV, Duong DM, Remenyik E, Hazarika P, Chuang A, Duvic M (1996) Interleukin-8 is induced in skin equivalents and is highest in those derived from psoriatic fibroblasts. *J Invest Dermatol* 107:615–21

Liu AY, Destoumieux D, Wong AV, Park CH, Valore EV, Liu L *et al.* (2002) Human beta-defensin-2 production in keratinocytes is regulated by interleukin-1, bacteria, and the state of differentiation. *J Invest Dermatol* 118:275–81

Lorenzo P, Bayliss MT, Heinegard D (1998) A novel cartilage protein (CILP) present in the mid-zone of human articular cartilage increases with age. *J Biol Chem* 273:23463–8

Marenholz I, Zirra M, Fischer DF, Backendorf Z, Ziegler A, Mischke D (2001) Identification of human epidermal differentiation complex (EDC)-encoded genes by subtractive hybridization of entire YACs to a gridded keratinocyte cDNA library. *Genomics* 11:341–55

Maretzky T, Reiss K, Ludwig A, Buchholz J, Scholz F, Proksch E *et al.* (2005) ADAM10 mediates E-cadherin shedding and regulates epithelial cell-cell adhesion, migration, and beta-catenin translocation. *Proc Natl Acad Sci USA* 102:9182–7

Mischke D, Korge BP, Marenholz I, Volz A, Ziegler A (1996) Genes encoding structural proteins of epidermal cornification and S100 calcium-binding proteins form a gene complex (''Epidermal Differentiation Complex'') on human chromosome 1q21. *J Invest Dermatol* 106:989–92

Norris RA, Damon B, Mironov V, Kasyanov V, Ramamurthi A, Moreno-Rodriguez R *et al.* (2007) Periostin regulates collagen fibrillogenesis and the biomechanical properties of connective tissues. *J Cell Biochem* 101:695–711

Ostendorff HP, Bossenz M, Mincheva A, Copeland NG, Gilbert DJ, Jenkins NA *et al.* (2000) Functional characterization of the gene encoding RLIM, the corepressor of LIM homeodomain factors. *Genomics* 69:120–30

Pascual M, Vicente M, Monferrer L, Artero R (2006) The Muscleblind family of proteins: an emerging class of regulators of developmentally programmed alternative splicing. *Differentiation* 74:65–80

Passerini AG, Polacek DC, Shi C, Francesco NM, Manduchi E, Grant GR *et al.* (2004) Coexisting proinflammatory and antioxidative endothelial transcription profiles in a disturbed flow region of the adult porcine aorta. *Proc Natl Acad Sci USA* 101:2482–7

Rosines E, Sampogna RV, Johkura K, Vaughn DA, Choi Y, Sakurai H *et al.* (2007) Staged *in vitro* reconstitution and implantation of engineered rat kidney tissue. *Proc Natl Acad Sci USA* 104:20938–43

Santoro MM, Gaudino G, Marchisio PC (2003) The MSP receptor regulates alpha6beta4 and alpha3beta1 integrins via 14-3-3 proteins in keratinocyte migration. *Dev Cell* 5:257–71

Saville MK, Sparks A, Xirodimas DP, Wardrop J, Stevenson LF, Bourdon JC *et al.* (2004) Regulation of p53 by the ubiquitin-conjugating enzymes UbcH5B/C *in vivo*. *J Biol Chem* 279:42169–81

Schroeder F, Zhou M, Swaggerty CL, Atshaves BP, Petrescu AD, Storey SM *et al.* (2003) Sterol carrier protein-2 functions in phosphatidylinositol transfer and signaling. *Biochemistry* 42:3189–202

Scott FL, Paddle-Ledinek JE, Cerruti L, Coughlin PB, Salem HH, Bird PI (1998) Proteinase inhibitor 6 (PI-6) expression in human skin: induction of PI-6 and a PI-6/proteinase complex during keratinocyte differentiation. *Exp Cell Res* 245:263–71

Shannon P, Markiel A, Ozier O, Baliga NS, Wang JT, Ramage D *et al.* (2003) Cytoscape: a software environment for integrated models of biomolecular interaction networks. *Genome Res* 13:2498–504

Simon M Jr, Juhasz I, Herlyn M, Hunyadi J (1996) Thrombospondin receptor (CD36) expression of human keratinocytes during wound healing in a SCID mouse/human skin repair model. *J Dermatol* 23:305–9

Smiley AK, Klingenberg JM, Aronow BJ, Boyce ST, Kitzmiller WJ, Supp DM (2005a) Microarray analysis of gene expression in cultured skin substitutes compared with native human skin. *J Invest Dermatol* 125:1286–301

Smiley AK, Klingenberg JM, Boyce ST, Supp DM (2005b) Keratin expression in cultured skin substitutes suggests that the hyperproliferative phenotype observed *in vitro* is normalized after grafting. *Burns* 32: 135–8

Spirin V, Mirny LA (2003) Protein complexes and functional modules in molecular networks. *Proc Natl Acad Sci USA* 100:12123–8

Subramanian A, Tamayo P, Mootha VK, Mukherjee S, Ebert BL, Gillette MA *et al.* (2005) Gene set enrichment analysis: a knowledge-based approach for interpreting genome-wide expression profiles. *Proc Natl Acad Sci USA* 102:15545–50

Supp DM, Supp AP, Bell SM, Boyce ST (2000) Enhanced vascularization of cultured skin substitutes genetically modified to overexpress vascular endothelial growth factor. *J Invest Dermatol* 114:5–13

Tasheva ES, Koester A, Paulsen AQ, Garrett AS, Boyle DL, Davidson HJ *et al.* (2002) Mimecan/osteoglycin-deficient mice have collagen fibril abnormalities. *Mol Vis* 8:407–15

Tremblay PL, Hudon V, Berthod F, Germain L, Auger FA (2005) Inosculation of tissue-engineered capillaries with the host's vasculature in a reconstructed skin transplanted on mice. *Am J Transplant* 5:1002–10

Tumbar T, Guasch G, Greco V, Blanpain C, Lowry WE, Rendl M *et al.* (2004) Defining the epithelial stem cell niche in skin. *Science* 303: 359–63

Turner FE, Broad S, Khanim FL, Jeanes A, Talma S, Hughes S *et al.* (2006) Slug regulates integrin expression and cell proliferation in human epidermal keratinocytes. *J Biol Chem* 281:21321–31

Wang J, Kirby CE, Herbst R (2002) The tyrosine phosphatase PRL-1 localizes to the endoplasmic reticulum and the mitotic spindle and is required for normal mitosis. *J Biol Chem* 277:46659–68

Webb A, Li A, Kaur P (2004) Location and phenotype of human adult keratinocyte stem cells of the skin. *Differentiation* 72:387–95

Wolf SE, Rose JK, Desai MH, Mileski JP, Barrow RE, Herndon DN (1997) Mortality determinants in massive pediatric burns. An analysis of 103 children with > or = 80% TBSA burns (> or = 70% full-thickness). *Ann Surg* 225:554–65

Xiao-Wu W, Herndon DN, Spies M, Sanford AP, Wolf SE (2002) Effects of delayed wound excision and grafting in severely burned children. *Arch Surg* 137:1049–54

Xie X, Lu J, Kulbokas EJ, Golub TR, Mootha V, Lindblad-Toh K *et al.* (2005) Systematic discovery of regulatory motifs in human promoters and 3′ UTRs by comparison of several mammals. *Nature* 434:338–45

Yang T, Espenshade PJ, Wright ME, Yabe D, Gong Y, Aebersold R *et al.* (2002) Crucial step in cholesterol homeostasis: sterols promote binding of SCAP to INSIG-1, a membrane protein that facilitates retention of SREBPs in ER. *Cell* 110:489–500

Yebra M, Montgomery AM, Diaferia GR, Kaido T, Silletti S, Perez B *et al.* (2003) Recognition of the neural chemoattractant Netrin-1 by integrins alpha6beta4 and alpha3beta1 regulates epithelial cell adhesion and migration. *Dev Cell* 5:695–707

Zigrino P, Steiger J, Fox JW, Loffek S, Schild A, Nischt R *et al.* (2007) Role of ADAM-9 disintegrin-cysteine-rich domains in human keratinocyte migration. *J Biol Chem* 282:30785–93